

# Ab Initio Study on the Kinetics of Hydrogen Abstraction for the H + Alkene → H<sub>2</sub> + Alkenyl Reaction Class

Lam K. Huynh,<sup>†</sup> Sylwester Panasewicz,<sup>‡</sup> Artur Ratkiewicz,<sup>‡</sup> and Thanh N. Truong<sup>\*,†</sup>

Department of Chemistry, University of Utah, 315 S. 1400 E. Rm. 2020, Salt Lake City, Utah 84112, and Chemistry Institute, University at Białystok, ul. Hurtowa 1 15-399 Białystok, Poland

Received: October 10, 2006; In Final Form: December 15, 2006

Kinetics of the hydrogen abstraction reaction class of the H + alkene has been studied using the reaction class transition state theory (RC-TST) combined with the linear energy relationship (LER) and the barrier height grouping (BHG) approach. The rate constants for the reference reaction, H + C<sub>2</sub>H<sub>4</sub>, were obtained by the canonical variational transition state theory (CVT) with the small curvature tunneling (SCT) correction in the temperature range of 300–3000 K. Combined with these data, both the RC-TST/LER, where only reaction energy is needed, and RC-TST/BHG, where no other information is needed, are found to be promising methods for predicting rate constants for a large number of reactions in this reaction class. Our analysis indicates that less than 50% systematic errors on the average exist in the predicted rate constants using the RC-TST/LER or RC-TST/BHG method while in comparison to explicit rate calculations the differences are less than 100% or a factor of 2 on the average.

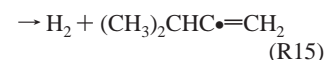
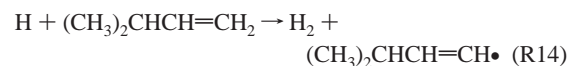
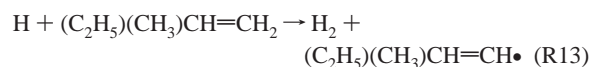
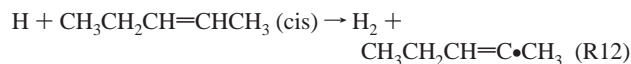
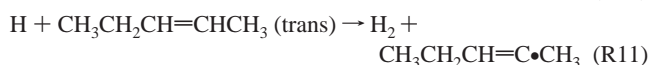
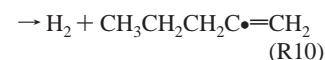
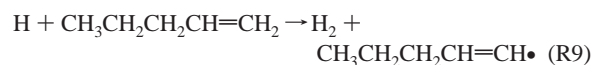
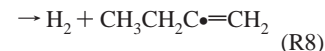
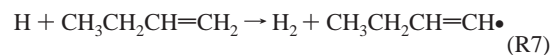
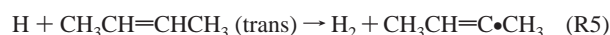
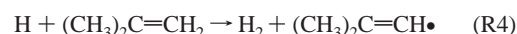
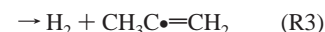
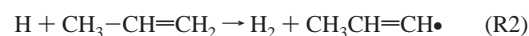
## 1. Introduction

The hydrogen abstraction reaction between a hydrogen atom and an alkene (C=C) to form a hydrogen molecule and an alkenyl (C=C•) radical is an important reaction class in combustion processes of hydrocarbon fuel.<sup>1</sup> For example, the reaction between a hydrogen atom and ethylene is an important source of the vinyl radical in flames which is an important intermediate in such processes. There are a number of indirect studies<sup>2–6</sup> though no direct measurements of the rate constants for the reaction. For reactions involving larger alkenes, even fewer data are available. For example, there are only two records for rate constants for reaction with propene. Rate constants for the reaction at the primary carbon site of the double bond are obtained by assuming that they are half of those of the reaction with ethylene; those for the other reaction are obtained by assuming the effect of methyl substitution to be the same as that in alkane.<sup>7</sup> Such approximations have not been validated. Recent developments and applications of the reaction class transition state theory (RC-TST)<sup>8–11</sup> indicated that it is possible to predict rate constants of any reaction in this reaction class, from *first-principles*, on the fly.

The aim of this study is to apply RC-TST for estimating rate constants of any arbitrary reaction in the H + alkenes → H<sub>2</sub> + alkenyl class. This is done by first deriving analytical correlation expressions for rate constants of the reference reaction with those in a small representative set of the class from explicit direct ab initio dynamics calculations of rate constants for all reactions in this representative set. The assumption is that these correlation expressions are applicable to all reactions in the class. So far, this assumption has shown to be valid.

To develop RC-TST parameters for the H + alkene class, 15 reactions including the reference reaction, i.e., the principal H + ethylene reaction, are considered as a representative set.

These reactions are given below:



where trans and cis denote trans and cis configurations for the carbon chain; here, carbon atoms with the dot sign represent the radical sites as in the products. Note that this set does not include reactions with resonance systems, e.g., 1,3-butadiene, as well as aromatic systems, e.g., benzene. The reason for this is given in the discussion section below.

\* E-mail: Truong@chem.chemistry.utah.edu.

<sup>†</sup> University of Utah.

<sup>‡</sup> University at Białystok.

## 2. Methodology

**Reaction Class Transition State Theory.** Since the details of the RC-TST method have been presented elsewhere,<sup>9,12–14</sup> we discuss only its main features here. It is based on the realization that reactions in the same class have the same reactive moiety; thus, the difference between the rate constants of any two reactions is mainly due to differences in the interactions between the reactive moiety and their different substituents. Within the RC-TST framework, the rate constant of an arbitrary reaction (denoted as  $k_a$ ) is proportional to the rate constant of a reference reaction,  $k_r$ , (Note that one often would choose the reference reaction to be the smallest reaction in the class, which is referred to as the principal reaction) in the same class by a temperature-dependent function  $f(T)$ :

$$k_a(T) = f(T) \times k_r(T) \quad (1)$$

The rate constants for the reference reaction are often known experimentally or can be calculated accurately from first-principles. The key idea of the RC-TST method is to factor  $f(T)$  into different components under the TST framework:

$$f(T) = f_\sigma \times f_\kappa \times f_Q \times f_V \quad (2)$$

where  $f_\sigma$ ,  $f_\kappa$ ,  $f_Q$ , and  $f_V$  are the symmetry number, tunneling, partition function, and potential energy factors, respectively. These factors are simply the ratios of the corresponding components in the TST expression for the two reactions:

$$f_\sigma = \frac{\sigma_a}{\sigma_r} \quad (3)$$

$$f_\kappa(T) = \frac{\kappa_a(T)}{\kappa_r(T)} \quad (4)$$

$$f_Q(T) = \frac{\left( \frac{Q_a^\ddagger(T)}{\Phi_a^R(T)} \right)}{\left( \frac{Q_r^\ddagger(T)}{\Phi_r^R(T)} \right)} = \frac{\left( \frac{Q_a^\ddagger(T)}{Q_r^\ddagger(T)} \right)}{\left( \frac{\Phi_a^R(T)}{\Phi_r^R(T)} \right)} \quad (5)$$

$$f_V(T) = \exp \left[ - \frac{(\Delta V_a^\ddagger - \Delta V_r^\ddagger)}{k_B T} \right] = \exp \left[ - \frac{\Delta \Delta V^\ddagger}{k_B T} \right] \quad (6)$$

$\sigma$  is the reaction symmetry number;  $\kappa(T)$  is the transmission coefficient accounting for the quantum mechanical tunneling effects;  $Q^\ddagger$  and  $\Phi^R$  are the total partition functions (per unit volume) of the transition state and reactants, respectively;  $\Delta V^\ddagger$  is the classical reaction barrier height;  $T$  is the temperature in Kelvin; and  $k_B$  and  $h$  are the Boltzmann and Planck constants, respectively. The potential energy factor can be calculated using the reaction barrier heights of the arbitrary reaction and the reference reaction. The classical reaction barrier height  $\Delta V^\ddagger$  for the arbitrary reaction can be obtained using the linear energy relationship (LER), similar to the well-known Evans–Polanyi linear free energy relationship,<sup>15–17</sup> between classical barrier heights and reaction energies of reactions in a given reaction class without having to calculate them explicitly. Alternatively, the barrier height for the arbitrary reaction can be obtained from the barrier height group (BHG) approach where all reactions in a subclass of reactions can be reasonably assumed to have the same barrier height.

The main tasks of this paper are (1) to determine the explicit expressions for these factors linking the rate constants of  $R_r$  and those of  $R_a$  in the same class using the representative set of reactions as mentioned earlier and (2) to provide error analyses of the results. Once these expressions are determined, thermal rate constants of any reaction in this class can be predicted from only the reaction energy needed for the LER expression and no other information is needed for the BHG approach.

**Computational details.** All the electronic structure calculations were carried out using the GAUSSIAN 3.0 program.<sup>18</sup> Hybrid nonlocal density functional theory (DFT), particularly Becke's half-and-half<sup>19</sup> (BH&H) nonlocal exchange and Lee–Yang–Parr<sup>20</sup> (LYP) nonlocal correlation functionals, has been found to be sufficiently accurate for predicting the transition state properties for hydrogen abstraction reactions by a radical.<sup>21–24</sup> Note that within the RC-TST framework, as discussed above, only the relative barrier heights are needed. Our previous studies have shown that the relative barrier heights can be accurately predicted by the BH&HLYP method.<sup>13,14</sup> Geometries of reactants, transition states, and products were optimized at the BH&HLYP level of theory with the Dunning's correlation-consistent polarized valence double- $\zeta$  basis set [3s2p1d/2s1p] denoted as cc-pVDZ,<sup>25</sup> which is sufficient to capture the physical change along the reaction coordinate for this type of reaction. Frequencies of the stationary points were also calculated at the same level of theory. This information was used to derive the RC-TST factors. The AM1 semiempirical method<sup>26</sup> was also employed to calculate the reaction energies of those reactions considered here. AM1 and BH&HLYP/cc-pVDZ reaction energies were then used to derive the LERs between the barrier heights and reaction energies. Note that the AM1 reaction energy is only used to extract accurate barrier height from the LERs, it is not directly involved in any rate calculations.

For the principal H + C<sub>2</sub>H<sub>4</sub> reaction, the minimum energy path (MEP) of the potential energy surface is also obtained at the BH&HLYP/cc-pVDZ level by following the Gonzalez–Schlegel steepest descent path<sup>27</sup> in the mass weighted Cartesian coordinates with a step size of 0.01 amu<sup>1/2</sup> bohr. Force constants at 34 selected points (17 points in the reactant channel and 17 points in the products channel from  $s = -1.0$ – $1.0$  amu<sup>1/2</sup> bohr) along the MEP were determined to obtain the necessary potential energy surface information for canonical variational transition state theory (CVT) calculations.<sup>28–30</sup> The points were chosen based on the curvatures of the MEP and the geometrical parameters as functions of the reaction coordinate according to our autofocusing technique.<sup>31</sup> Energetic information along the MEP is further refined by single point calculation using the coupled cluster method including single and double excitations with a quasi-perturbative triples contribution [CCSD(T)]<sup>32</sup> with the cc-pVTZ basis set at the BH&HLYP/cc-pVDZ geometry, which is denoted as [CCSD(T)/cc-pVTZ//BH&HLYP/cc-pVDZ]. The CCSD(T) energies, combined with the BH&HLYP/cc-pVDZ geometries and frequencies, were then used for rate constant calculations.

To derive the RC-TST correlation functions, TST/Eckart rate constants for all reactions in the above representative reaction set were calculated employing the kinetic module of the web-based Computational Science and Engineering Online (CSE-Online) environment.<sup>33</sup> In these calculations, overall rotations were treated classically and vibrations were treated quantum mechanically within the harmonic approximation except for the modes corresponding to the internal rotations of the CH<sub>3</sub> groups, which were treated as the hindered rotations using the method

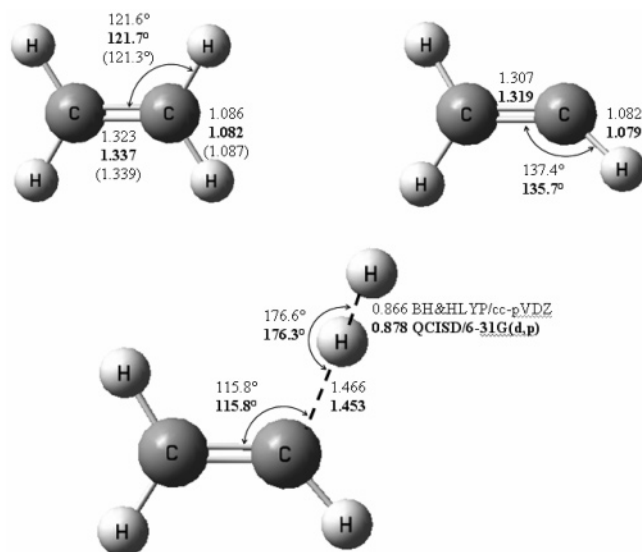


**Figure 1.** Optimized geometries (distances in angstroms and angles in degrees) of the reactant  $C_2H_4$ , product  $C_2H_3$ , and transition state at the BH&HLYP/cc-pVDZ and QCISD/6-31G(d,p) (bold numbers) levels. The numbers in parentheses are the experimental values (ref 35).

suggested by Ayala et al.<sup>34</sup> Thermal rate constants were calculated for the temperature range of 300–3000 K, which is sufficient for many combustion applications such as premixed flame and shock-tube simulations.

### 3. Results and Discussion

In the discussion below, the rate constants for the principal reaction are presented first and then we describe how the RC-TST factors were derived using the training reaction set. Subsequently, several error analyses were performed in order to provide some estimates on the accuracy of the RC-TST method applied to this reaction class. The first error analysis is the direct comparison between the calculated rate constants with those available in the literature for the  $R_2$  and  $R_3$  reactions. The second error analysis is the comparison between rate constants obtained from the RC-TST method and those from explicit full TST/Eckart calculations for the whole training set. The final analysis is on the systematic errors caused by introducing approximations in the RC-TST correlation functions.

The first task for applying the RC-TST method to any reaction class is to have rate constants of the reference reaction as accurate as possible. In this study, the principal reaction is chosen as the reference reaction. Because of its small size, its rate constants can be calculated accurately using the canonical variational transition state theory (CVT) with the small curvature tunneling (SCT) method for the temperature range of 300–3000 K.

**3.1. Rate Constants of the Reference  $H + C_2H_4 \rightarrow H_2 + C_2H_3$  Reaction.** *3.1.1. Stationary Points.* The optimized geometrical parameters of the reactant ( $C_2H_4$ ), product ( $C_2H_3$ ), and the transition state at the BH&HLYP/cc-pVDZ and QCISD/6-31G(d,p) levels of theory are shown in Figure 1. The available experimental data are also given in parentheses.<sup>35</sup> The transition state was confirmed by normal-mode analysis to have only one imaginary frequency whose mode corresponds to the transfer of the hydrogen atom between  $C_2H_4$  and the H atom. From Figure 1, it is seen that the BH&HLYP/cc-pVDZ method gives optimized geometries close to those from the QCISD/6-31G(d,p) level of theory for the reactants, products, and transition state with the largest difference being 0.013 Å. These data are

**TABLE 1: Calculated Barrier Height and Reaction Energy for the  $H + C_2H_4$  Reaction (numbers are in kilocalories per mole)<sup>a</sup>**

level of theory	$\Delta E$	$\Delta V^\ddagger$
BH&HLYP/cc-pVDZ	5.54	13.05
CCSD(T)/cc-pVTZ//BH&HLYP/cc-pVDZ	5.92	15.74
QCISD/6-31G(d,p)	7.04	19.14
MP4/6-31G**//MP2/6-31G** (ref 4)	6.5	15.06

<sup>a</sup> Zero-point energy correction is included.

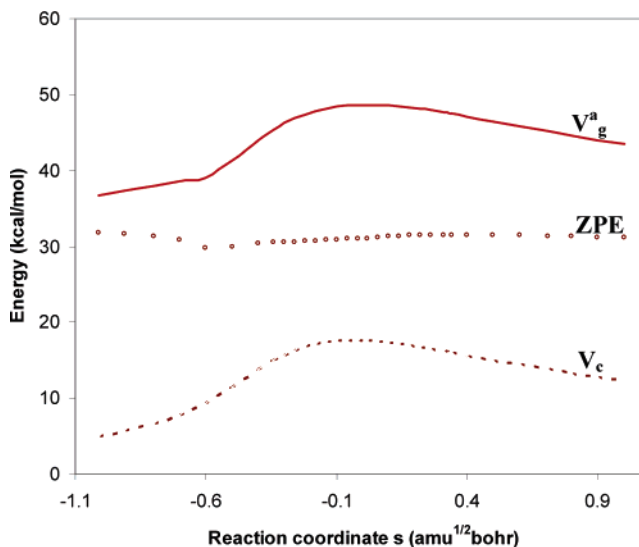


**Figure 2.** Potential energy surface for the reaction  $H + C_2H_4$  in the vicinity of the transition state.  $V_g^a$  is the vibrationally adiabatic ground state potential curve,  $V_c$  is the classical adiabatic ground state potential curve, and ZPE is the vibrational zero-point energy.

very close to experimental data for the  $C_2H_4$  reactant. For the frequency calculation, the results from BH&HLYP/cc-pVDZ are consistent with the QCISD/6-31G(d,p) level with the average absolute difference of about  $60 \text{ cm}^{-1}$ . This leads to differences in the total zero-point energies (ZPEs) of 0.31, 0.24, and 0.17 kcal/mol for reactants, transition state, and products, respectively. Consequently, the differences between the two levels on the ZPE corrections on the classical barrier and reaction energy are insignificant, i.e., less than 0.1 kcal/mol. The barrier height and reaction energy with the inclusion of the ZPE correction calculated at various levels of theory are listed in Table 1. It is believed that the CCSD(T)/cc-pVTZ//BH&HLYP/cc-pVDZ gives accurate energetic data, and in fact, the data are consistent with those reported by Kynazev et al.<sup>4</sup> with the difference in the barrier height being about 0.5 kcal/mol. It is noted that calculated  $\Delta H_{\text{rxn}}^\circ$  (298 K) of 7.6 kcal/mol at the BH&HLYP/cc-pVDZ level is reasonably close to the experimental data of 6.9 kcal/mol.<sup>36</sup>

To compromise accuracy and computational efficiency, the CCSD(T)/cc-pVTZ//BH&HLYP/cc-pVDZ method is used to correct the energy along the minimum energy path for the  $H + C_2H_4$  reaction for rate calculations below. Figure 2 is the potential energy surface for this reaction where the classical adiabatic ground state potential curve  $V_c$  was obtained from CCSD(T)/cc-pVTZ//BH&HLYP/cc-pVDZ, zero-point energy (ZPE) was calculated using BH&HLYP/cc-pVDZ frequencies, and the vibrationally adiabatic ground state potential curve  $V_g^a$  was the sum product of the two previous terms  $V_c + \text{ZPE}$ . The ZPE profile is rather flat in the vicinity of the transition state, and thus, the shapes of the  $V_c$  and  $V_g^a$  are very similar. The ZPE lowers the classical barrier height and reaction energy about 1.8 and 2.9 kcal/mol, respectively.

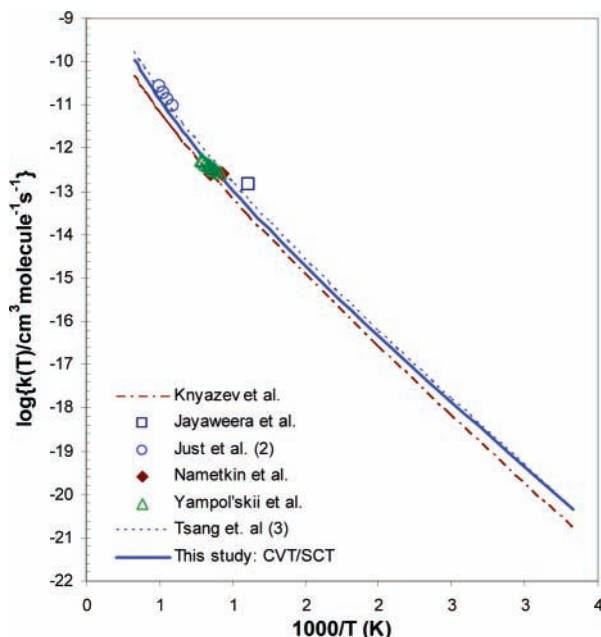


**Figure 3.** Arrhenius plots of the calculated and available rate constants for the H + C<sub>2</sub>H<sub>4</sub> → H<sub>2</sub> + C<sub>2</sub>H<sub>3</sub>. The numbers in parentheses are uncertainty factors.

**3.1.2. Rate Constants.** The rate constants of the forward reactions were calculated using the canonical variational transition state theory (CVT) with small curvature tunneling (SCT) in a wide temperature range of 300–3000 K. Geometries and vibrational frequencies at the selected points along the MEP at the BH&HLYP level were used. The corresponding energy is from CCSD(T)/cc-pVTZ//BH&HLYP/cc-pVDZ. The reaction symmetry number of 4 is used to account for the number of symmetrically equivalent reaction paths. The CVT/SCT rate constants were plotted in Figure 3 and fitted to an Arrhenius expression, given as follows:

$$k_f = 2.102 \times 10^{-19} \times T^{2.752} \times \exp\left(-\frac{5862}{T}\right),$$

cm<sup>3</sup>/(molecule · s) (7)

The available rate constants in the literature are also given in Figure 3. The numbers in parentheses are uncertainty factors. The value of a given rate constant, *k*, could lie between *k<sub>m</sub>/f* and *k<sub>m</sub>f*, where *k<sub>m</sub>* is the reported value and *f* is an uncertainty factor.

Knyazev et al.<sup>4</sup> combined the TST kinetics model with ab initio calculations and the experimental data in the temperature range 499–497 K for the reverse reaction, H<sub>2</sub> + C<sub>2</sub>H<sub>3</sub>, to derive the rate constants for this reaction in the temperature range of 200–3000 K. These data are lower than ours by less than a factor of 2 for the whole temperature range, which is within the uncertainty limits of the data. Our calculated rate constants are within the accuracy of the suggested data from Just et al. (in the temperature range of 1700–2200 K),<sup>3</sup> from Yampol'skii et al. (1093–1213 K),<sup>6</sup> and Nametkin et al. (1073 and 1173 K).<sup>5</sup> Jayaweera et al.<sup>2</sup> obtained the rate constants for this reaction at 900 K and pressures of 150–580 torr relatively through the two reactions, H + C<sub>2</sub>H<sub>4</sub> → C<sub>2</sub>H<sub>5</sub> and C<sub>2</sub>H<sub>5</sub> + C<sub>2</sub>H<sub>4</sub> → C<sub>2</sub>H<sub>3</sub> + C<sub>2</sub>H<sub>6</sub>, thus introducing a large uncertainty. Tsang et al.<sup>37</sup> suggested slightly higher data with a large uncertainty of a factor of 3 based on a bond energy–bond order fit to the data of Just et al.<sup>3</sup> and the reaction thermochemistry. It can be seen that our calculated data are in good agreement with those available in

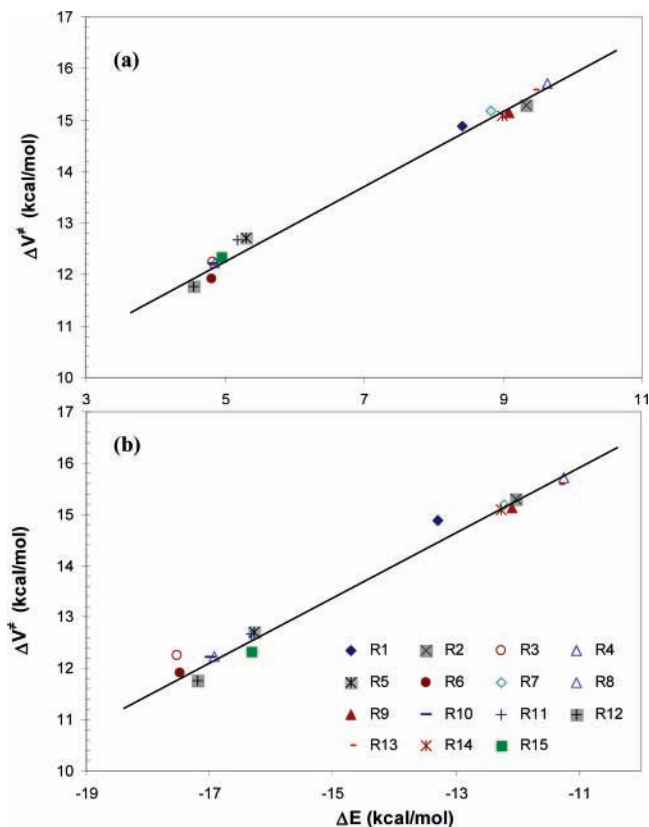


**Figure 4.** Linear energy relationship plots of the barrier heights, Δ*V*<sup>‡</sup>, versus the reaction energies, Δ*E*. Barrier heights were calculated at the BH&HLYP/cc-pVDZ level of theory. Δ*E* values were calculated at the (a) BH&HLYP/cc-pVDZ and (b) AM1 levels of theory.

the literature; thus, they will be used for estimating the rate constants for reactions in this reaction class.

**3.2 Reaction Class Parameters.** In the discussion below, we first describe how the RC-TST factors were derived using the above training set. Subsequently, several error analyses were performed in order to provide some estimates on the accuracy of the RC-TST method applied to this reaction class. The first error analysis is the direct comparison between the calculated rate constants with those available in the literature for reactions R<sub>2</sub> and R<sub>3</sub>. The second error analysis is the comparison between rate constants calculated by the RC-TST method and those from explicit full TST/Eckart calculations for the whole training set. The final analysis is on the systematic errors caused by introducing approximations in order to derive analytical expressions for the correlation functions.

**3.2.1. Calculation of the Potential Energy Factor.** The potential energy factor can be calculated using eq 6, where Δ*V*<sub>a</sub><sup>‡</sup> and Δ*V*<sub>r</sub><sup>‡</sup> are the barrier heights of the arbitrary and reference reactions, respectively. We have also shown that within a given class there is a linear energy relationship (LER) between the barrier height and the reaction energy, similar to the well-known Evans-Polanyi linear free energy relationship.<sup>15–17</sup> Thus, with an LER, accurate barrier heights can be predicted from only the reaction energies. In this study, the LER is determined where the reaction energy can be calculated by either the AM1 or the BH&HLYP level of theory. Moreover, for this reaction class, it is found that the barrier heights can also be grouped together into two groups: (i) primary carbon sites of the double bond and (ii) secondary carbon sites (see Figure 4). This can be referred to as barrier height grouping (BHG). It can be seen that the substitute of an alkyl group will stabilize the radical products, thus lowering the barrier heights. For this

**TABLE 2: Classical Reaction Energies, Barrier Heights, and Absolute Deviations between Calculated Barrier Heights from DFT and Semiempirical Calculations and Those from LER Expressions and the BHG Approach<sup>b</sup>**

rxn	$\Delta E$		$\Delta V^\ddagger$				$ \Delta V^\ddagger - \Delta V_{\text{estimated}}^\ddagger ^f$		
	DFT <sup>a</sup>	AM1 <sup>b</sup>	DFT <sup>a</sup>	DFT <sup>c</sup>	AM1 <sup>d</sup>	BHG <sup>e</sup>	DFT <sup>c</sup>	AM1 <sup>d</sup>	BHG <sup>e</sup>
R <sub>1</sub>	8.42	-3.30	14.88	14.80	14.48	15.34	0.08	0.40	0.46
R <sub>2</sub>	9.33	-12.03	15.29	15.46	15.26	15.34	0.17	0.03	0.05
R <sub>3</sub>	4.82	-17.52	12.25	12.22	11.89	12.26	0.03	0.36	0.01
R <sub>4</sub>	9.64	-11.25	15.70	15.68	15.74	15.34	0.03	0.04	0.36
R <sub>5</sub>	5.31	-16.27	12.71	12.57	12.66	12.26	0.14	0.06	0.45
R <sub>6</sub>	4.81	-17.48	11.91	12.22	11.91	12.26	0.31	0.00	0.35
R <sub>7</sub>	8.83	-12.22	15.18	15.10	15.15	15.34	0.08	0.03	0.17
R <sub>8</sub>	4.86	-16.92	12.24	12.25	12.26	12.26	0.02	0.02	0.03
R <sub>9</sub>	9.09	-12.09	15.13	15.28	15.22	15.34	0.15	0.09	0.21
R <sub>10</sub>	4.83	-16.98	12.22	12.23	12.22	12.26	0.01	0.00	0.05
R <sub>11</sub>	5.19	-16.33	12.67	12.48	12.62	12.26	0.18	0.05	0.41
R <sub>12</sub>	4.56	-17.20	11.76	12.04	12.09	12.26	0.27	0.32	0.50
R <sub>13</sub>	9.44	-11.32	15.58	15.54	15.70	15.34	0.04	0.12	0.23
R <sub>14</sub>	8.99	-12.27	15.08	15.22	22.08	22.01	0.14	0.04	0.26
R <sub>15</sub>	4.95	-16.32	12.33	12.32	23.69	23.83	0.01	0.29	0.07
MAD <sup>g</sup>							0.11	0.12	0.24

<sup>a</sup> Calculated at the BH&HLYP/cc-pVDZ level of theory. <sup>b</sup> Calculated at the AM1 level of theory. <sup>c</sup> Calculated from the LER using reaction energies calculated at the BH&HLYP/cc-pVDZ level of theory: eq 8a. <sup>d</sup> Calculated from the LER using reaction energies calculated at the AM1 level of theory: eq 8b. <sup>e</sup> Estimated from barrier height grouping. <sup>f</sup>  $\Delta V^\ddagger$  from BH&HLYP/cc-pVDZ calculations;  $\Delta V_{\text{estimated}}^\ddagger$  from the linear energy relationship using BH&HLYP/cc-pVDZ and AM1 reaction energies or from barrier height grouping. <sup>g</sup> Mean absolute deviations (MAD) for reactions R<sub>2</sub>–R<sub>15</sub>. <sup>h</sup> Zero-point energy correction is not included. Energies are in kilocalories per mole.

reason, the reactions at the secondary carbon of the double bond have a barrier height about 3 kcal/mol, lower than those at the primary site.

The reaction energies and barrier heights for all representative reactions in the training set are given explicitly in Table 2. The observed linear energy relationships plotted against the reaction energies calculated at the BH&HLYP/cc-pVDZ and AM1 levels are shown in Figure 4a and b, respectively. These linear fits were obtained using the least-square fitting method and have the following expressions:

$$\Delta V^\ddagger = 0.7173 \times \Delta E^{\text{BH\&HLYP}} + 8.77 \text{ (kcal/mol)} \quad (8a)$$

$$\Delta V^\ddagger = 0.6143 \times \Delta E^{\text{AM1}} + 22.65 \text{ (kcal/mol)} \quad (8b)$$

The absolute deviations of reaction barrier heights between the LERs and the direct DFT BH&HLYP/cc-pVDZ calculations are smaller than 0.3 kcal/mol (see Table 2). The mean absolute deviation of reaction barrier heights predicted from BH&HLYP and AM1 reaction energies are 0.11 and 0.12 kcal/mol, respectively. These deviations are in fact smaller than the systematic errors of the computed reaction barriers from full electronic structure calculations. Note that in the RC-TST/LER methodology only the relative barrier height is needed. To compute these relative values, the barrier height of the reference reaction R<sub>1</sub>, calculated at the same level of theory, i.e., BH&HLYP/cc-pVDZ, is needed and has the value of 14.88 kcal/mol (see Table 2).

It is noted that reactions with resonance systems, e.g., 1,3-butadiene, as well as aromatic systems, e.g., benzene, are not included in this study. It is expected that the aromatic system behaves differently, and it was addressed by our previous study.<sup>38</sup> For the nonaromatic resonance systems, it is found that the LER relationship is excellent at the BH&HLYP level but is not as good at the AM1 level of theory. However, if one is interested in rate constants for such reactions, the AM1 should be excluded.

On the basis of the observation of barrier heights grouping (BHG) on the two reaction sites, the average values are assigned to all reactions in the same type of site, particularly 15.34 and 12.26 kcal/mol for primary and secondary carbon sites of the

double bond, respectively. The maximum and the averaged deviations of reaction barrier heights estimated from this grouping are 0.45 and 0.24 kcal/mol, respectively. Therefore, this approach can be used to estimate the relative barrier height quickly with an acceptable deviation. The key advantage of this approach is that it does not require any other information to estimate rate constants.

In conclusion, the barrier heights for any reaction in this reaction class can be obtained by using either the LER or BHG approach. The estimated barrier height is then used to calculate the potential energy factor using eq 6. The performance of both approaches is discussed in the error analyses below.

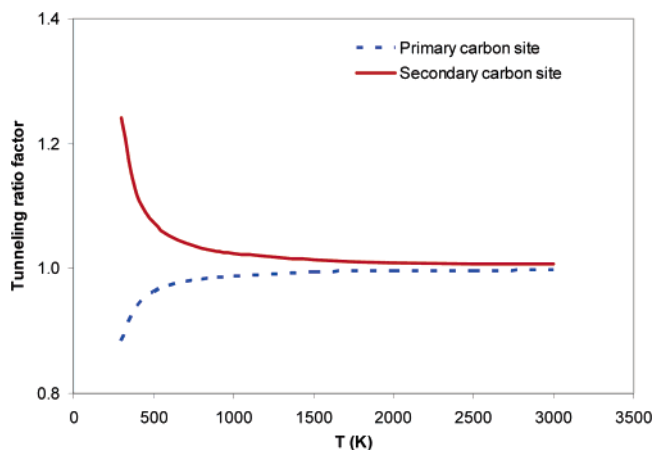
**3.2.2. Calculation of the Symmetry Number Factor.** The symmetry number factors  $f_\sigma$  were calculated simply from the ratio of reaction symmetry numbers of the arbitrary and reference reactions using eq 3 and are listed in Table 3. The reaction symmetry number of a reaction is given by the number of symmetrically equivalent reaction paths. It can be easily calculated from the rotational symmetry numbers of the reactant and the transition state;<sup>31</sup> thus, this factor can be calculated exactly.

**3.2.3. Calculation of the Tunneling Factor.** The tunneling factor  $f_k$  is the ratio of the transmission coefficient of reaction R<sub>a</sub> to that of reaction R<sub>r</sub>. Due to the cancellation of errors in calculations of the tunneling factors, we have shown that the factor  $f_k$  can be reasonably estimated using the one-dimension Eckart method.<sup>39</sup> Calculated results for the representative set of reactions can then be fitted to an analytical expression. It is known that the tunneling coefficient depends on the barrier height. We have shown that the barrier heights group together into two groups, namely primary and secondary of the double-bond carbons (see the Calculation of the Potential Energy Factor section); it is expected that reactions in the same group have the same tunneling factor, and thus, the average value can be used for the whole group. Simple expressions for the two tunneling factors for primary and secondary carbon sites of the double bond are obtained by fitting to the average calculated values and are given below:

**TABLE 3: Calculated Symmetry Number Factors and Tunneling Factors at 300 K**

rxn	symmetry no. factor	tunneling ratio factor, $f_k$			
		Eckart <sup>a</sup>	fitting <sup>b</sup>	deviation <sup>c</sup>	% deviation <sup>d</sup>
R <sub>1</sub>	1.00	4.10 <sup>f</sup>			
R <sub>2</sub>	0.50	0.88	0.88	0.01	0.6
R <sub>3</sub>	0.25	1.26	1.23	0.04	2.9
R <sub>4</sub>	0.50	0.85	0.88	0.04	4.2
R <sub>5</sub>	0.50	1.20	1.23	0.02	2.0
R <sub>6</sub>	0.50	1.18	1.23	0.05	4.4
R <sub>7</sub>	0.50	0.90	0.88	0.02	1.7
R <sub>8</sub>	0.25	1.27	1.23	0.04	3.4
R <sub>9</sub>	0.50	0.90	0.88	0.01	1.5
R <sub>10</sub>	0.25	1.35	1.23	0.12	9.1
R <sub>11</sub>	0.25	1.20	1.23	0.03	2.2
R <sub>12</sub>	0.25	1.21	1.23	0.02	1.7
R <sub>13</sub>	0.50	0.87	0.88	0.02	2.1
R <sub>14</sub>	0.50	0.91	0.88	0.02	2.5
R <sub>15</sub>	0.25	1.26	1.23	0.03	2.4
MAD <sup>e</sup>				0.03	2.9

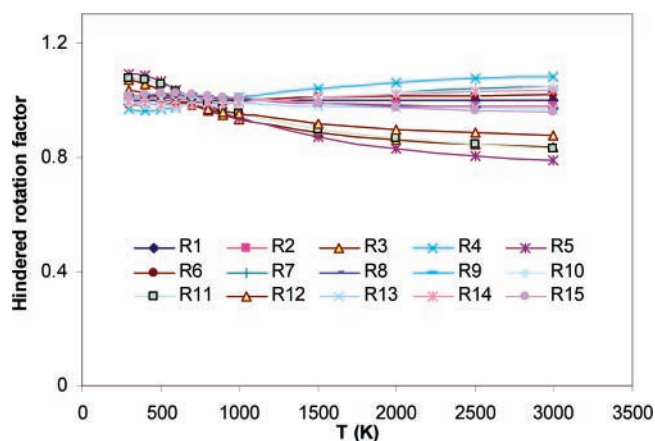
<sup>a</sup> Calculated directly using the Eckart method with the BH&HLYP/cc-pVDZ reaction barrier heights and energies. <sup>b</sup> Calculated by using a fitting expression (see eqs 9a and 9b). <sup>c</sup> Absolute deviation between the fitting and directly calculated values. <sup>d</sup> Percentage deviation (%). <sup>e</sup> Mean absolute deviations (MAD) and deviation percentage between the fitting and directly calculated values. <sup>f</sup> Tunneling coefficient calculated for reaction (R<sub>1</sub>) using the Eckart method with the energetic and frequency information at BH&HLYP/cc-pVDZ.

**Figure 5.** Plots of the tunneling ratio factors  $f_k$  as a function of temperature for abstractions of hydrogen from primary (dotted line) and secondary (solid line) carbon sites of the double bond.

$$f_k = 0.99 - 0.64 \times \exp\left[-\frac{T}{166}\right] \quad \text{for primary carbon sites} \quad (9a)$$

$$f_k = 1.02 + 1.44 \times \exp\left[-\frac{T}{155}\right] \quad \text{for secondary carbon sites} \quad (9b)$$

The correlation coefficients for these fits are larger than 0.999. The three equations are plotted in Figure 5. Table 3 also lists the error analysis of tunneling factors at 300 K. It can be seen that the same tunneling factor expression can be reasonably assigned to those reactions at the same site with the largest absolute deviation of 0.12 and the largest percentage deviation of 9% for R<sub>10</sub>; also, the mean absolute deviation is 3%, compared to the direct Eckart calculation using reaction information from the BH&HLYP/cc-pVDZ level of theory. At higher temperatures, tunneling contributions to the rate constants decrease and thus, as expected, the differences between the approximated values and the explicitly calculated ones also

**Figure 6.** Effect of the hindered rotation treatment to the total rate constants for all reactions in the temperature range 300–3000 K.

decrease; for example, the maximum error for all reactions is less than 1% at 500 K.

**3.2.4. Calculation of Partition Function Factor.** The total partition factor is the product of the translational, rotational, and vibrational partition factors. The translational and rotational factors are temperature-independent and are generally not unity. As pointed out in our previous study,<sup>9</sup> the temperature-dependent part of the total partition function factor  $f_Q$  mainly originates from the vibrational factor due to the differences in the coupling between the substituents with the reactive moiety as well as the existence of internal rotation motions in large alkenes. For this reaction class, the rotations of the alkyl groups along the C–C bond at some reactants, transition states, and products needs to be treated as hindered rotations rather than as vibrations. We used the approach proposed by Ayala et al.<sup>34</sup> for treating hindered rotations. Note that the principal reaction R<sub>1</sub> does not have such internal rotations. The effect of the hindered rotation treatment on the total rate constants can be seen in Figure 6. It can be seen that the contribution of such a treatment only amount at most 20% of the total rate constants. Therefore, for simplicity, the influence of these hindered rotation factors can be ignored in the RC-TST approach. This will introduce some errors which will be included in the systematic error of the method.

The total partition function factors for 14 reactions were plotted in Figure 7. It can be seen that the variations in these factors are small, and thus, it is reasonable to assume that the averaged value from the training set can be applied to the whole class. The average values are fitted into an analytical expression as given below:

$$f_Q = 0.47 - 0.32 \times \exp\left[-\frac{T}{314}\right] \quad (10)$$

**3.2.5. Prediction of Rate Constants.** What we have established so far are the necessary parameters—namely, the potential energy factor, the symmetry number factor, the tunneling factor, and the partition function factor—for application of the RC-TST theory to predict rate constants for any reaction in the H + alkene class. The procedure for calculating rate constants of an arbitrary reaction in this class is as follows: (i) Calculate the potential energy factor using eq 6 with the  $\Delta V_r^\ddagger$  value of 14.88 kcal/mol. The reaction barrier height can be obtained using the LER approach by employing eq 8a for BH&HLYP/cc-pVDZ or eq 8b for AM1 reaction energies or by the BHG approach. (ii) Calculate the symmetry number factor from eq 3 or see Table 3. (iii) Compute the tunneling factor using eqs 9a and 9b for primary and secondary carbon sites, respectively. (iv) Evaluate

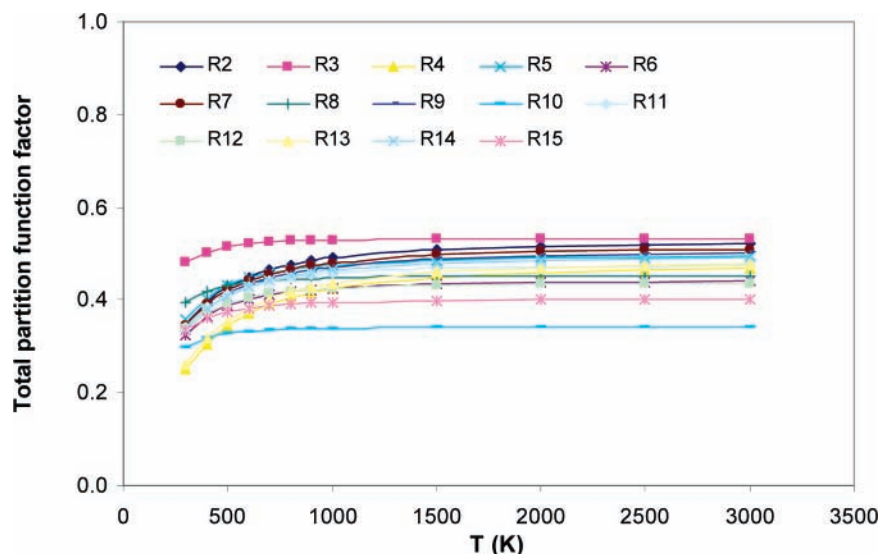


Figure 7. Plots of the total partition function factor for 14 reactions, R<sub>2</sub>–R<sub>15</sub>.

TABLE 4: Parameters and Formulations of the RC-TST Method for the H + Alkene → H<sub>2</sub> + Alkenyl Reaction Class (H + C<sub>2</sub>H<sub>4</sub> is the Reference Reaction)

	$k(T) = f_{\sigma} \times f_k(T) \times f_Q(T) \times f_V(T) \times k_r(T); f_V(T) = \exp[-(\Delta V^{\ddagger} - \Delta V_r^{\ddagger})/k_B T]$	
	T is in kelvin; $\Delta V^{\ddagger}$ and $\Delta E$ are in kilocalories per mole; zero-point energy correction is not included	
	calculated explicitly from the symmetry of reactions (see Table 3)	
$f_{\sigma}$		
$f_k(T)$	$f_k = 0.99 - 0.64 \times \exp[-(T/166)]$	for primary carbon sites
	$f_k = 1.02 + 1.44 \times \exp[-(T/155)]$	for secondary carbon sites
$f_Q(T)$	$f_Q = 0.47 - 0.32 \times \exp[-(T/314)]$	
$\Delta V^{\ddagger}$	LER	$\Delta V^{\ddagger} = 0.7173 \times \Delta E^{\text{BH\&HLYP}} + 8.77$
		$\Delta V^{\ddagger} = 0.6143 \times \Delta E^{\text{AM1}} + 22.65$
	$\Delta V_r^{\ddagger} = 14.88 \text{ kcal/mol}^a$	
$k_r(T)$ (eq 7)	$k_r = 2.102 \times 10^{-19} \times T^{2.752} \times \exp(-5862/T)$	cm <sup>3</sup> /(molecule·s)
BHG approach	$k(T) = 1.117 \times 10^{-19} \times T^{2.66} \times \exp[-6307/T]$	for primary carbon sites
	$k(T) = 2.214 \times 10^{-20} \times T^{2.77} \times \exp[-4574/T]$	for secondary carbon sites

<sup>a</sup> Calculated value for the reaction R<sub>2</sub> at the BH&HLYP/cc-pVDZ level of theory.

the partition function factor using eq 10. (v) Finally, the rate constants of the arbitrary reaction can be calculated by taking the product of the reference reaction rate constant given by eq 7 with the reaction class factors above. Table 4 summarizes the RC-TST parameters for this reaction class.

As mentioned above, the barrier heights can be roughly approximated by the BHG approach (see section 3.2.1). If the BHG barrier heights and average values for other factors are used, the rate constants are denoted by RC-TST/BHG. The RC-TST/BHG rate constants for any reactions belonging to this class can be estimated without any further calculations as:

$$k(T) = 1.117 \times 10^{-19} \times T^{2.66} \times \exp\left[-\frac{6307}{T}\right]$$

for primary carbon sites (11a)

$$k(T) = 2.214 \times 10^{-20} \times T^{2.77} \times \exp\left[-\frac{4574}{T}\right]$$

for secondary carbon sites (11b)

Because the primary carbon sites have two hydrogen atoms which can be reasonably considered equivalent in some cases and the secondary sites only have one hydrogen atom, the symmetry factors of 2 and 1 are also included in the two rate constant expressions above.

To illustrate the theory, we selected two reactions R<sub>2</sub> and R<sub>3</sub> whose rate constants have been suggested from a literature review. It is noted that there is no previous theoretical calculation or direct experimental data available for these reactions. Figure 8a and b show the predicted rate constants of reactions R<sub>2</sub> and

R<sub>3</sub> using the RC-TST method and suggested data.<sup>7</sup> In the figure, the “RC-TST exact” notation means that the reaction class factors were calculated explicitly within the TST/Eckart framework rather than using the approximate expressions listed in Table 4. Since the barrier heights obtained from either BH&HLYP/cc-pVDZ or AM1 energies are similar, we can expect their rate constants to be similar.

For these two reactions, the rate constants calculated using the RC-TST/LER are not much different from those of RC-TST/BHG for these two reactions. Though, for other reactions, the difference might be larger. The RC-TST predicts values lower than the suggested data from Tsang et al.<sup>7</sup> It is noted that Tsang et al. assumed that the rate expression for the abstraction of vinylic hydrogen (R<sub>2</sub>) is half of the rate expression for hydrogen atom attack on ethylene presented in the same report (or see Figure 3) which is higher than that of our reference reaction, while the effect of methyl substitution is assumed to be the same as that in alkane for reaction R<sub>3</sub>. According to our analysis that the rate constants for reaction R<sub>2</sub> are much lower than those of the principal reaction, particularly by a factor of 6.2 and 3 at 300 and 2500 K, respectively. This comparison only gives a qualitative picture about the performance of this approach since there is a large uncertainty in the reported rate constants for these two reactions.

The accuracy of the RC-TST rate constants depends on several factors. At the fundamental level, it depends on the validity of the transition state theory approximations on which the RC-TST method is based and the semiclassical tunneling (SCT) approximations which are used for the reference (or

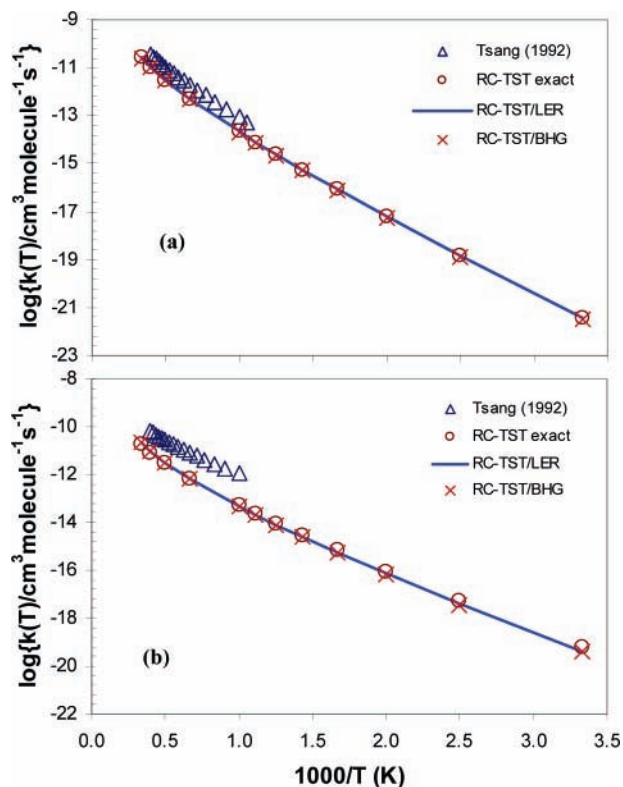


**Figure 8.** Arrhenius plots of the calculated rate constants using the RC-TST methods for two representative hydrogen abstraction reactions along with the available literature values: (a) H + C<sub>3</sub>H<sub>6</sub> at primary carbon and (b) H + C<sub>3</sub>H<sub>6</sub> at secondary carbon. Only the reaction energies at the BH&HLYP/cc-pVDZ level used for the LER were presented.

principal) reaction. In addition, it depends on the accuracy of all approximations that were introduced so that explicit calculations of the transition state structure and frequency are not required. The related errors will be referred to as systematic errors and are discussed below.

A better analysis on the efficiency of the RC-TST method would be to compare the RC-TST results with explicit theoretical calculations. As mentioned in our previous studies,<sup>9,13,14</sup> the RC-TST methodology can be thought of as a procedure for

extrapolating rate constants of the reference reaction to those of any given reaction in the class. Comparisons between the calculated rate constants for a small number of reactions using both the RC-TST and the full TST/Eckart methods would provide additional information on the accuracy of the RC-TST method. To be consistent, the TST/Eckart rate constants of the reference reaction were used in calculation of RC-TST rate constants for this particular analysis rather than using the expression in eq 7. The results for this error analysis for 14 representative reactions (i.e., the comparisons between the RC-TST/LER and full TST/Eckart methods) are shown in Figure 9. Here, we plotted the relative deviation defined by  $(|k^{\text{TST/Eckart}} - k^{\text{RC-TST/LER}}|/k^{\text{TST/Eckart}})$  as a percent versus the temperature for all reactions in the training set, R<sub>2</sub>–R<sub>15</sub>. The relative errors are less than 50% for all test cases; thus, it can be concluded that the RC-TST can predict thermal rate constants for reactions in this class within a factor of 2 when compared to those calculated explicitly using the TST/Eckart method. It is noted that this analysis is presented for the RC-TST/LER only. One would expect a similar or a slightly worse performance for the RC-TST/BHG approach.

Finally, we examined the systematic errors in different factors in the RC-TST/LER and the RC-TST/BHG methods. The total error is affected by the errors in the approximations in the potential energy factor, tunneling factor, and partition function factor introduced in the method. It is noted that the symmetry number factor is “exact”, but the error for the partition function factor does include the error in the approximation for the hindered rotation treatment. The deviations/errors between the approximated and exact factors within the TST framework are calculated at each temperature for every reaction in the training set and then averaged over the whole class. For the LER approach, the error in the potential energy factor comes from the use of an LER expression as in eqs 8a and 8b, that of the tunneling factor, from using the two eqs 9a–9b, and that of the partition function factor, from using eq 10. The results of the analysis on the errors from different relative rate factors, namely,  $f_{\text{tr}}$ ,  $f_{\text{Q}}$ , and  $f_{\text{v}}$ , used in the RC-TST method are shown in Figure 10. It is noted that the effect of neglecting the hindered rotation treatment was also included in the error for the total factor. The results with the RC-TST/BHG (denoted as BHG) are also included in this figure. The error for the potential energy factor

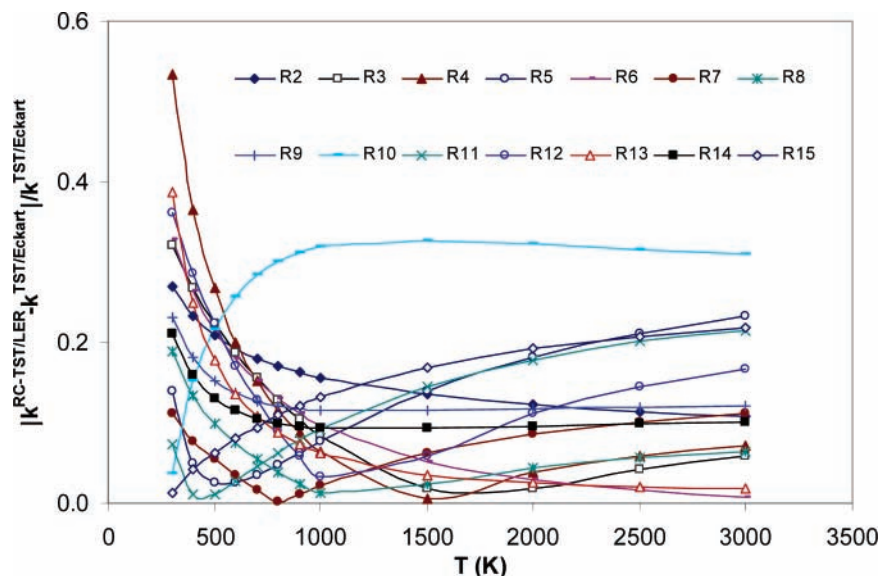


**Figure 9.** Relative absolute deviations as functions of the temperature between rate constants calculated from the RC-TST/LER and full TST/Eckart methods for all selected reactions. BH&HLYP reaction energies were used for the LER.

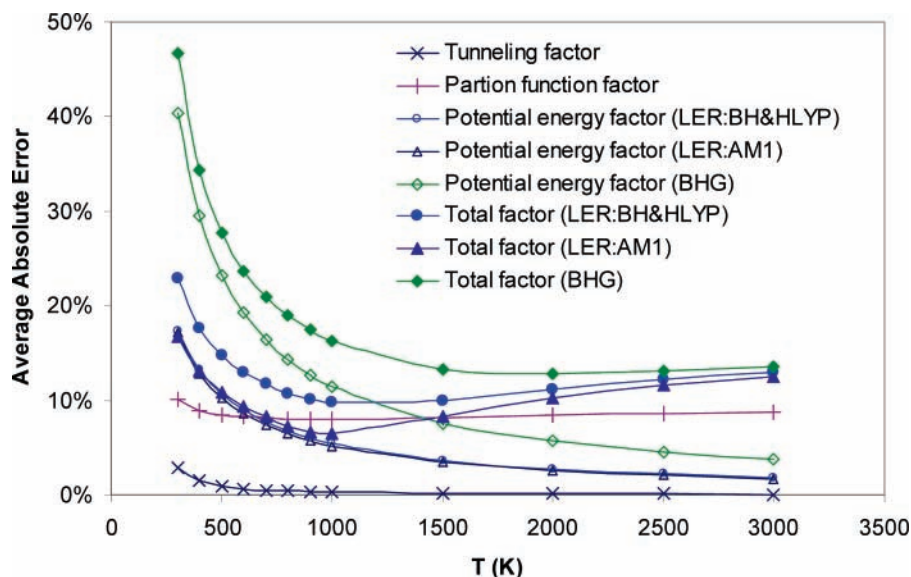


**Figure 10.** Averaged absolute errors of the total relative rate factors  $f(T)$  (eq 2) and its components, namely, the tunneling ( $f_t$ ), partition function ( $f_p$ ), and potential energy ( $f_v$ ) factors, as functions of temperature. It is noted that the effect of hindered rotation treatment was also included in the total relative rate factors.

arises from using the average barrier heights for primary and secondary carbon sites (BHG approximation). The total error is from the use of the expressions 11a and 11b for the primary and secondary sites, respectively. In this figure, we plotted the absolute errors averaged over all 14 reactions,  $R_2$ – $R_{15}$  as a function of temperature.

It can be seen that the absolute error decreases with the temperature increase with the exception of the total errors for the LER with both BH&HLYP and AM1, which show a small increase when the temperature rises in the temperature range of 1000–3000 K. This can be explained by the effect of neglecting the hindered rotation treatment (see Figure 6) where the hindered rotation treatment is more important in the same temperature range.

Of the factors, the tunneling and partition function factors show the least temperature-dependent errors for the whole temperature range. The tunneling factor introduced the largest error of less than 3%, while the partition factor gives an error of less than 10%. The errors in  $f_v$  from using the BH&HLYP and AM1 are very similar (less than 20%), and both are much smaller than those from using the BHG approach. At higher temperatures, the absolute difference between the two approaches (LER vs BHG) decreases.

The total systematic errors due to the use of simple analytical expressions for different reaction class factors are less than 50% in the temperature range 300–3000 K. The total error is less than 25% for the LER approach with both BH&HLYP and AM1 reaction energies, while BHG has the largest error of 50% at 300 K. If accurate rate constants are needed, the RC-TST/LER is recommended, while the BHG gives a quick estimation without doing any additional calculation.

#### 4. Conclusion

We have extended our application of the reaction class transition state theory combined with the linear energy relationship and the barrier height grouping approach to the prediction of thermal rate constants for hydrogen abstraction reactions of the  $H + \text{alkene}$  class. The rate constants for the reference reaction,  $H + C_2H_4$ , were obtained by the CVT/SCT method in the temperature range 300–3000 K. Combined with these data, the RC-TST/LER, where only reaction energy is needed,

and RC-TST/BHG, where no other information is needed, are both found to be promising methods for predicting rate constants for a large number of reactions in a given reaction class. Our analysis indicates that less than 50% systematic errors, on the average, exist in the predicted rate constants using the RC-TST/LER or RC-TST/BHG method, while in comparison to explicit rate calculations the differences are less than 100% or a factor of 2 on the average.

**Acknowledgment.** This work is supported in part by the National Science Foundation. L.K.H. is grateful to the Vietnam Education Foundation for a Graduate Fellowship. The authors also acknowledge the Utah Center for High Performance Computing for computing resources and support.

#### References and Notes

- (1) Warnatz, J. *Combustion Chemistry*; Gardiner, W. C., Jr., Ed.; Springer-Verlag: New York, 1984.
- (2) Jayaweera, I. S.; Pacey, P. D. *Int. J. Chem. Kinet.* **1988**, *20*, 719.
- (3) Just, T.; Roth, P.; Damm, R. *Symp. (Int.) Combust. Proc.* **1977**, *16*, 961.
- (4) Knyazev, V. D.; Bencsura, A.; Stoliarov, S. I.; Slagle, I. R. *J. Phys. Chem.* **1996**, *100*, 11346.
- (5) Nametkin, N. S.; Shevel'kova, L. V.; Kalinenko, R. A. *Dokl. Chem.* **1975**, *221*, 239.
- (6) Yampol'skii, Y. P. *Kinet. Catal.* **1974**, *15*, 532.
- (7) Tsang, W. *Ind. Eng. Chem. Res.* **1992**, *31*, 3.
- (8) Huynh, L. K.; Ratkiewicz, A.; Truong, T. N. *J. Phys. Chem. A* **2006**, *110*, 473.
- (9) Zhang, S.; Truong, T. N. *J. Phys. Chem. A* **2003**, *107*, 1138.
- (10) Kungwan, N.; Truong, T. N. *J. Phys. Chem. A* **2005**, *109*, 7742.
- (11) Huynh, L. K.; Zhang, S.; Truong, T. N. *Proc. Combust. Inst.* **2006**, in press.
- (12) Truong, T. N.; Duncan, W. T.; Tirtowidjojo, M. *Phys. Chem. Chem. Phys.* **1999**, *1*, 1061.
- (13) Truong, T. N. *J. Chem. Phys.* **2000**, *113*, 4957.
- (14) Truong, T. N.; Maity, D. K.; Truong, T. T. *J. Chem. Phys.* **2000**, *112*, 24.
- (15) Evans, M. G.; Polanyi, M. *Proc. R. Soc.* **1936**, *154*, 133.
- (16) Evans, M. G.; Polanyi, M. *Trans. Faraday Soc.* **1936**, *32*, 1333.
- (17) Polanyi, J. C. *Acc. Chem. Res.* **1972**, *5*, 161.
- (18) Frisch, M. J.; Trucks, G. W.; Schlegel, H. B.; Scuseria, G. E.; Robb, M. A.; Cheeseman, J. R.; Montgomery, J. A., Jr.; T. V.; Kudin, K. N.; Burant, J. C.; Millam, J. M.; Iyengar, S. S.; Tomasi, J.; Barone, V.; Mennucci, B.; Cossi, M.; Scalmani, G.; Rega, N.; Petersson, G. A.; Nakatsuji, H.; Hada, M.; Ehara, M.; Toyota, K.; Fukuda, R.; Hasegawa, J.; Ishida, M.; Nakajima, T.; Honda, Y.; Kitao, O.; Nakai, H.; Klene, M.; Li, X.; Knox, J. E.; Hratchian, H. P.; Cross, J. B.; Adamo, C.; Jaramillo, J.;

Gomperts, R.; Stratmann, R. E.; Yazyev, O.; Austin, A. J.; Cammi, R.; Pomelli, C.; Ochterski, J. W.; Ayala, P. Y.; Morokuma, K.; Voth, G. A.; Salvador, P.; Dannenberg, J. J.; Zakrzewski, V. G.; Dapprich, S.; Daniels, A. D.; Strain, M. C.; Farkas, O.; Malick, D. K.; Rabuck, A. D.; Raghavachari, K.; Foresman, J. B.; Ortiz, J. V.; Cui, Q.; Baboul, A. G.; Clifford, S.; Cioslowski, J.; Stefanov, B. B.; Liu, G.; Liashenko, A.; Piskorz, P.; Komaromi, I.; Martin, R. L.; Fox, D. J.; Keith, T.; Al-Laham, M. A.; Peng, C. Y.; Nanayakkara, A.; Challacombe, M.; Gill, P. M. W.; Johnson, B.; Chen, W.; Wong, M. W.; Gonzalez, C.; Pople, J. A. *Gaussian 03*, revision A.1; Gaussian, Inc.: Pittsburgh, PA, 2003.

- (19) Becke, A. D. *J. Chem. Phys.* **1993**, *98*, 1372.
- (20) Lee, C.; Yang, W.; Parr, R. G. *Phys. Rev.* **1988**, *37*, 785.
- (21) Truong, T. N. *J. Chem. Phys.* **1994**, *100*, 14.
- (22) Truong, T. N.; Duncan, W. *J. Chem. Phys.* **1994**, *101*, 7408.
- (23) Lynch, B. J.; Fast, P. L.; Harris, M.; Truhlar, D. G. *J. Phys. Chem. A* **2000**, *104*, 4811.
- (24) Zhang, Q.; Bell, R.; Truong, T. N. *J. Phys. Chem.* **1995**, *99*, 592.
- (25) Dunning, T. H., Jr. *J. Chem. Phys.* **1989**, *94*, 5523.
- (26) Dewar, M.; Thiel, W. *J. Am. Chem. Soc.* **1977**, *99*, 2338.
- (27) Gonzalez, C.; Schlegel, H. B. *J. Phys. Chem.* **1990**, *94*, 5523.
- (28) Truhlar, D. G.; Garrett, B. C. *Acc. Chem. Res.* **1980**, *13*, 440.
- (29) Truhlar, D. G.; Isaacson, A. D.; Garrett, B. C. *Theory of Chemical Reaction Dynamics*; Baer, M., Ed.; CRC Press: Boca Raton, Florida, 1985; Vol. 4, p 65.

(30) Truhlar, D. G. Direct dynamics method for the calculation of reaction rates. In *The Reaction Path in Chemistry: Current Approaches and Perspectives*; Heidrich, D., Ed.; Kluwer Academic: Norwell, MA, 1995; p 229.

(31) Duncan, W. T.; Bell, R. L.; Truong, T. N. *J. Comput. Chem.* **1998**, *19*, 1039.

(32) Pople, J. A.; Head-Gordon, M.; Raghavachari, K. *J. Chem. Phys.* **1987**, *87*, 5968.

(33) Truong, T. N.; Nayak, M.; Huynh, H. H.; Cook, T.; Mahajan, P.; Tran, L.-T. T.; Bharath, J.; Jain, S.; Pham, H. B.; Boonyasiriwat, C.; Nguyen, N.; Andersen, E.; Kim, Y.; Choe, S.; Choi, J.; Cheatham III, T. E.; Facelli, J. C. *J. Chem. Inf. Model.* **2006**, *46*, 971.

(34) Ayala, P. Y.; Schlegel, H. B. *J. Chem. Phys.* **1998**, *108*, 2314.

(35) Lide, D. R. *CRC Hand Book of Chemistry and Physics*, 80th ed.; CRC Press: Boca Raton, FL, 1999–2000.

(36) NIST Standard Reference Database Number 69. <http://webbook.nist.gov/chemistry> (June 2005 release).

(37) Tsang, W.; Hampson, R. F. *J. Phys. Chem. Ref. Data* **1986**, *15*, 1087.

(38) Violi, A.; Truong, T. N.; Sarofim, A. F. *J. Phys. Chem. A* **2004**, *108*, 4846.

(39) Miller, W. H. *J. Am. Chem. Soc.* **1979**, *101*, 6810.